Astron. Astrophys. 363, 660–666 (2000)

ASTRONOMY AND ASTROPHYSICS

Orbital elements of barium stars formed through a wind accretion scenario

J.H. Liu[1,2], **B. Zhang**[1,5], **Y.C. Liang**[3], **and Q.H. Peng**[4,5]

[1] Department of Physics, Hebei Normal University, Shijiazhuang 050016, P.R. China
[2] Department of Physics, Shijianzhuang Teachers' College, Shijiazhuang 050041, P.R. China
[3] Beijing Astronomical Observatory, Chinese Academy of Sciences, Beijing 100012, P.R. China
[4] Department of Astronomy, Nanjing University, Nanjing 210093, P.R. China
[5] Chinese Academy of Sciences – Peking University Joint Beijing Astrophysical Center, Beijing 100871, P.R. China

Received 3 July 2000 / Accepted 11 September 2000

Abstract. Taking the total angular momentum conservation in place of the tangential momentum conservation, and considering the square and higher power terms of orbital eccentricity e, the changes of orbital elements of binaries are recalculated for wind accretion scenario. These new equations of orbital elements are used to calculate the properties of barium stars. Our results show that, during the evolution of a binary system, the system widens as it loses mass, and the orbital period increases, while orbital eccentricity remains nearly constant, which can quantitatively explain the observed (e,log$P$) properties of normal G, K giants and those of barium stars. The results reflect the evolution from G, K giant binaries to barium binaries, namely, the orbits of barium stars have been modified by the mass-transfer process responsible for their chemical peculiarities, whereas most of the G, K giant binaries are probably pre-mass transfer binaries. Moreover, the results showed that the barium stars with longer orbital period P>1600 days may be formed by accreting part of the ejecta from the intrinsic AGB stars through wind accretion, while those with shorter orbital period may be formed through dynamically stable late case C mass transfer or common envelope ejection.

Key words: stars: late-type – stars: chemically peculiar – stars: AGB and post-AGB – stars: mass-loss – stars: binaries: spectroscopic – accretion, accretion disks

1. Introduction

Extrinsic AGB stars include various classes of G- and K-type barium stars and those cooler S and C stars in which ^{99}Tc ($\tau_{\frac{1}{2}}$=2×10^5 yr) is not observed. It is generally believed that they belong to binary systems and their heavy-element overabundance come from accretion of the mass ejected by their companions (the former AGB stars, now evolved into white dwarfs) (McClure et al. 1980; Boffin & Jorissen 1988; Jorissen & Mayor 1992; Jorissen & Van Eck 2000; Jorissen et al. 1998; Böhm-Vitense et al. 2000; Karakas et al. 2000). The mass exchange took place about 1×10^6 years ago, so the ^{99}Tc produced in the original thermal pulse AGB (hereafter TP-AGB) stars have practically all decayed. The accretion may either be disk accretion (Iben & Tutukov 1985) or common envelope ejection (Paczynski 1976). Han et al. (1995) detailedly investigated the evolutionary channels for the formation of barium stars.

Boffin & Jorissen (1988) calculated quantitatively the variations of orbital elements caused by wind accretion in binary systems. They also estimated the heavy-element overabundance of barium stars. In a subsequent paper (Boffin & Začs 1994), the heavy-element overabundance of barium stars was calculated using the same technique, and the correlation with orbital period was interpreted. The calculated results were compared with the observations (Začs 1994). In our calculation of the overabundance (Chang et al. 1997), we considered the variation in the binary separation, $\delta r\neq0$, and combined the nucleosynthesis scenario of intrinsic TP-AGB stars (Zhang et al. 1998) with the scenario of successive pulsed accretion and mixing of wind mass.

Some important conclusions have been obtained in the theory of wind accretion, but previous calculations on orbital elements were not very reliable because of the neglect of the $\delta r/r$ term and the adoption of tangential momentum conservation (Chang et al. 1997 and references therein). For the rotating binary system with wind mass loss, total angular momentum conservation is a more realistic assumption than tangential momentum conservation. Also, for the sake of simplicity, previous calculations regarded orbital eccentricity as $e\ll1$ (Huang 1956; Boffin & Jorissen 1988; Theuns et al. 1996). Observations show that the eccentricities of almost half of all barium stars are too large to be neglected, with the largest observed value = 0.97 (Jorissen et al. 1998). Thus the assumption of $e\ll1$ for the barium star systems is not valid.

The (e,log$P$) diagram is a very useful tool to study binary evolution given the abundant information contained in it. For example, the distributions of orbital period P with the eccentricity of progenitor systems correlate with the final characteristics of binary systems through mass accretion. Generally, barium stars

Send offprint requests to: Y.C. Liang (lyc@yac.bao.ac.cn)

evolved from normal red giant binary systems. Observations show that the orbital eccentricities of Ba stars are smaller than those of the G, K giants from open clusters, and the (e,log$P$) diagrams of the two systems show strong correlation (Jorissen & Boffin 1992; Boffin et al. 1993; Jorissen et al. 1998; Jorissen 1999). Few quantitative calculations have been put into this correlation though they are very important to understanding the binary evolution.

In this paper, we adopt the hypothesis that the total angular momentum is conserved, and we do not neglect the square and the higher power terms of eccentricity, in order to recalculate the change equations of orbital elements of binary systems caused by stellar wind accretion. Then these new equations are used to calculate the properties of barium stars produced by this mechanism. Hence we quantitatively explain the observed relations between the (e,log$P$) diagram of normal G, K giants and that of barium stars. In Sect. 2, we analyze the properties of (e,log$P$) diagrams of barium stars and normal G, K giants. In Sect. 3, we present the angular momentum conservation model of the wind accretion. Our results and analysis are illustrated in Sect. 4. And in Sect. 5, we draw some conclusions and discuss the results.

2. The (e,log$P$) diagram

The observations of the G, K giants from open cluster and barium stars are the same as in Jorissen et al. (1998), and are given in our Figs. 1 and 2 respectively. Analyzing the observations, we can understand the properties of them as following.

(1) At any given orbital period, the maximum eccentricity found among barium systems is much smaller than for cluster giants. And the average eccentricity of barium stars is generally smaller than that of cluster giants. The average orbital eccentricity of barium stars is 0.14, while the corresponding mean value of cluster giant is 0.23 (Boffin et al. 1993).

(2) In the two (e,log$P$) diagrams, the maximum eccentricity line of barium system is almost parallel to the corresponding maximum eccentricity line of cluster giants. It seems that the maximum eccentricity line of cluster giants is moved in a parallel way with the increase of orbital period to reach the barium systems. Boffin et al. (1993) exhibited this character.

(3) In the (e,log$P$) diagrams, the average eccentricity line of barium stars is almost parallel to the corresponding line of cluster giants. It seems that the latter is moved in a parallel way to the longer period region to reach the barium systems.

(4) In the (e,log$P$) diagram of normal G, K giants, the maximum orbital period for a circular orbit is $\sim$350 days; while the maximum orbital period for a circular orbit is $\sim$2000 days in the (e,log$P$) diagram of barium stars, which is longer than the corresponding threshold of cluster giants. The (e,log$P$) diagrams of S and CH stars are very similar to those of barium stars (Jorissen et al. 1998).

(5) Although, at a given orbital period, the maximum eccentricity found among barium systems is much smaller than for cluster giants. Still, the (e,log$P$) diagram of barium systems shows that quite large eccentricities are found among barium stars, and the highest value is up to 0.97 (HD 123949), yet at large periods ($P\sim$9200 days for HD 123949).

The reasonable binary evolutionary model of orbital elements should quantitatively explain the above mentioned observational properties.

3. The angular momentum conservation model of wind accretion scenario

For the binary system, the two components (an intrinsic AGB star with mass M_1, the present white dwarf star, and a main sequence star with mass M_2, the present barium star) rotating around the mass core C, so the total angular momentum is conserved in the mass core reference frame. If the two components exchange material through wind accretion, the angular momentum conservation of the total system is shown by:

$$\Delta(\mu r^2\dot{\theta}) = \omega r_1^2(\Delta M_1 + \Delta M_2) + r_2 v(\Delta M_1 + \Delta M_2), \quad (1)$$

where μ is reduced mass, and r is the distance from M_2 to M_1. r_1, r_2 are the distances from M_1, M_2 to the mass core C respectively. ω(=$2\pi/P$, P=$2\pi A^2(1-e^2)^{\frac{1}{2}}/h$, is orbital period) is angular velocity. v is an additional effective velocity defined through the angular momentum variation in the direction of orbital motion of component 2. The first term on the right side of the equal-sign is the angular momentum lost by the escaping material, and the second term is the additional angular momentum lost by the escaping material.

Using the methods similar to those adopted by Huang (1956) and Boffin & Jorissen (1988), but considering the angular momentum conservation of the total system and not neglecting the square and higher power terms of eccentricity, we can obtain the formulas for the changes in the orbital elements:

$$\begin{aligned}\frac{\Delta A}{A} &= -2(1-e^2)^{\frac{1}{2}}\left[\frac{\Delta M_1}{M_1}+\frac{\Delta M_2}{M_2}-\frac{\Delta M_1+\Delta M_2}{M_2}\frac{v}{v_{\rm orb}}\right] \\ &\quad + 2(1-e^2)^{\frac{1}{2}}\frac{M_2(\Delta M_1+\Delta M_2)}{M_1(M_1+M_2)} \\ &\quad + [2(1-e^2)^{\frac{1}{2}}-1]\frac{\Delta M_1+\Delta M_2}{M_1+M_2}, \end{aligned} \quad (2)$$

$$\begin{aligned}\frac{e\Delta e}{1-e^2} &= [1-(1-e^2)^{\frac{1}{2}}]\left[\frac{\Delta M_1}{M_1}+\frac{\Delta M_2}{M_2}-\frac{\Delta M_1+\Delta M_2}{M_1+M_2}\right] \\ &\quad - [1-(1-e^2)^{\frac{1}{2}}]\frac{M_2(\Delta M_1+\Delta M_2)}{M_1(M_1+M_2)} \\ &\quad - \frac{3e^2}{2(1-e^2)^{\frac{1}{2}}}\frac{\Delta M_1+\Delta M_2}{M_2}\frac{v}{v_{\rm orb}}, \end{aligned} \quad (3)$$

where A is the semi-major axis of the relative orbit of component 2 around 1, and e is the orbital eccentricity (more details can be found in Appendix). Here, we take $v=0$ (Boffin & Jorissen 1988).

For the mass being accreted by the barium star, we use the Bondi-Hoyle accretion rate (Theuns et al. 1996; Jorissen et al. 1998):

$$\Delta M_2^{\rm acc} = -\frac{\alpha}{A^2}\left[\frac{GM_2}{v_{\rm ej}^2}\right]^2\left[\frac{1}{1+(v_{\rm orb}/v_{\rm ej})^2}\right]^{\frac{3}{2}}\Delta M_1, \quad (4)$$

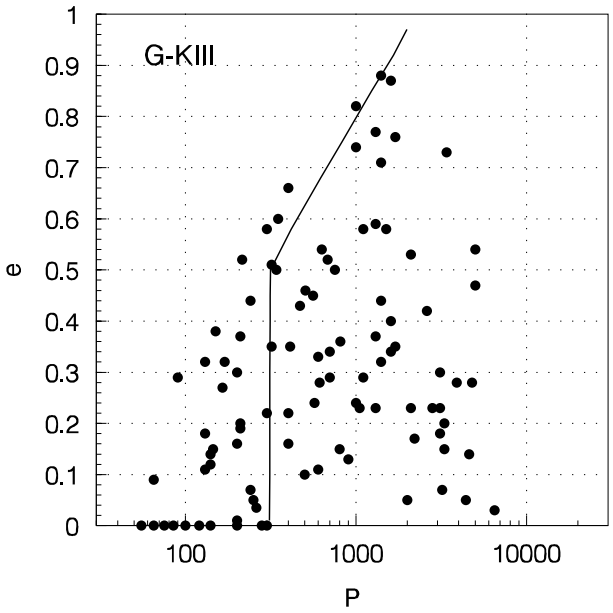

Fig. 1. The (e,log$P$) diagram for the G and K giants. The solid represents the maximum orbital eccentricity line of red giant binaries.

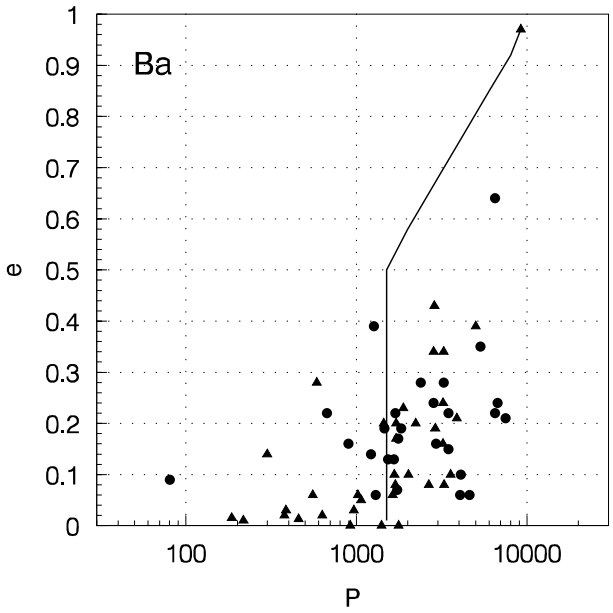

Fig. 2. The (e,log$P$) diagram for barium stars. The solid represents the calculated maximum orbital eccentricity of barium star systems created by the wind accretion scenario.

where α is a constant expressing the accretion efficiency, and $\alpha\sim$0.05 in the situation of interest here according to the detailed hydrodynamic simulations (Theuns et al. 1996; Jorissen et al. 1998). e is the orbital eccentricity. $v_{\rm ej}$ is the wind velocity and $v_{\rm orb}$ is the orbital mean velocity. After fixing the initial conditions, for the mass ΔM_1, ejected at each pulse by the primary star, we can solve the Eqs. (2)$-$(4) for ΔM_2, the mass accreted by the secondary star. The final mass and critical Roche lobe radii of the intrinsic AGB stars, and the initial envelope mass of the extrinsic AGB stars are all calculated using the same formulas as in Boffin & Jorissen (1988) in which the mass ratio is $q = M_1/M_2$.

4. Results and analysis

Adopting the wind accretion scenario above mentioned, we calculate the orbital elements of barium systems. We take as standard case: $M_{1,0}$=3.0$M_\odot$, $M_{2,0}$=1.3$M_\odot$, $v_{\rm ej}$=15 km s^{-1} (Boffin & Začs 1994). The results are shown in Figs. 1$-$4 and Table 1.

According to the suggestions of Jorissen et al. (1998) and Zhang et al. (1999), the barium stars with longer orbital periods ($P>$1500 d and $P>$1600 d respectively) are formed through stellar wind accretion scenario. So we adopt 1600 days to be the lower bound of wind accretion for the formation of barium stars in our calculation. Fig. 1 show the maximum eccentricities line of the normal giants (solid line), which is regarded as the initial orbit of the binary system. The observations are for the G, K giants in open cluster (Mermilliod 1996; Jorissen et al. 1998). While the solid line in Fig. 2 represents the calculated eccentricity of barium stars through our wind accretion model, which is near to the observed maximum eccentricities line of barium stars.

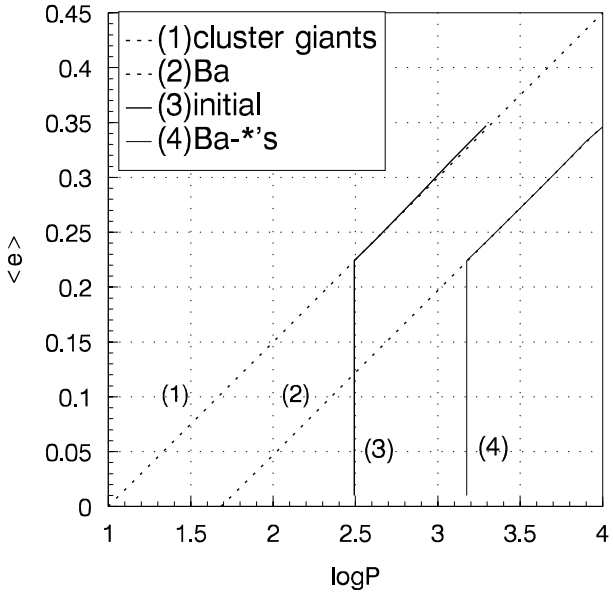

Fig. 3. Mean eccentricity$-$log$P$ diagram for binary systems. The dashed line (1) represents the fit of mean eccentricity of observed cluster giants taken from Boffin et al. (1993), and the dashed line (2) represents the corresponding fit of mean eccentricity of observed Ba stars. The thin solid line (4) represents the orbital eccentricity of barium stars with η=0.685 in Eq. (11) of Boffin et al. (1993), and the thick solid line (3) represents the corresponding initial eccentricity of binary systems.

Fig. 3 show the (e,log$P$) results about mean orbital eccentricities. The dashed line (1) represents the fit of mean eccentricity of observed cluster giants, which is taken from Boffin et al. (1993); the dashed line (2) represents the fit of mean eccentricity of observed barium stars taken from Boffin et al. (1993). The

Table 1. Variations of the eccentricity e during the process of mass loss by wind as a function of the mass ratio q for the different initial eccentricities. The initial eccentricities are 0.1, 0.3, 0.5 and 0.75 respectively.

q	e			
	$e_0 = 0.1$	$e_0 = 0.3$	$e_0 = 0.5$	$e_0 = 0.75$
2.31	0.1	0.3	0.5	0.75
2.21	0.1001	0.3002	0.5003	0.7503
2.11	0.1001	0.3004	0.5007	0.7506
2.01	0.1002	0.3006	0.5010	0.7508
1.91	0.1003	0.3008	0.5013	0.7511
1.81	0.1004	0.3010	0.5016	0.7513
1.72	0.1004	0.3012	0.5019	0.7516
1.62	0.1005	0.3014	0.5022	0.7518
1.52	0.1005	0.3016	0.5025	0.7520
1.43	0.1006	0.3017	0.5027	0.7522
1.33	0.1006	0.3019	0.5029	0.7524
1.24	0.1007	0.3020	0.5031	0.7525
1.14	0.1007	0.3020	0.5032	0.7526
1.05	0.1007	0.3021	0.5033	0.7527
1.00	0.1007	0.3021	0.5033	0.7527
0.86	0.1007	0.3020	0.5032	0.7526
0.77	0.1006	0.3019	0.5030	0.7525
0.68	0.1006	0.3017	0.5026	0.7522
0.59	0.1005	0.3013	0.5020	0.7519
0.50	0.1003	0.3008	0.5012	0.7513
0.41	0.1000	0.3001	0.5000	0.7506

thin solid line (4) represents the orbital eccentricity of barium stars with $\eta = 0.685$ in Eq. (11) of Boffin et al. (1993) (Boffin & Jorissen (1988) predicted values of η in the range 0.3 to about 1). In calculation, we firstly fix the eccentricity of barium stars at given periods (thin solid line (4)), then use our wind accretion model to determine the corresponding initial eccentricity of binary systems (thick solid line (3)), which nearly overlap the observed mean values of cluster giants (dashed line (1)).

These results for the (e,log$P$) diagrams show that the barium stars indeed evolve from the G, K giants, and the properties of barium stars with longer orbital periods (P>1600 d) can be explained by the wind accretion scenario.

Table 1 reports the variations of the eccentricities e during the process of mass loss by wind as a function of mass ratio q (q=M_1/M_2) for different initial eccentricities of binary systems. The initial eccentricities are 0.1, 0.3, 0.5 and 0.75 respectively. The results show that e is very nearly constant in the course of the wind accretion, which is different from the result of Theuns et al. (1996).

Fig. 4 shows the evolution of the Roche radius due to mass loss via the wind as a function of the mass ratio q=M_1/M_2 for different final orbital periods (in unit of days) of barium systems. The results show that, for a given final period of a barium star, the mass loss through stellar wind leads to the increase of the Roche radius, thus making Roche lobe overflow (hereafter RLOF) more difficult to achieve. Moreover, the longer final orbital period, the larger Roche radius will be obtained, hence it

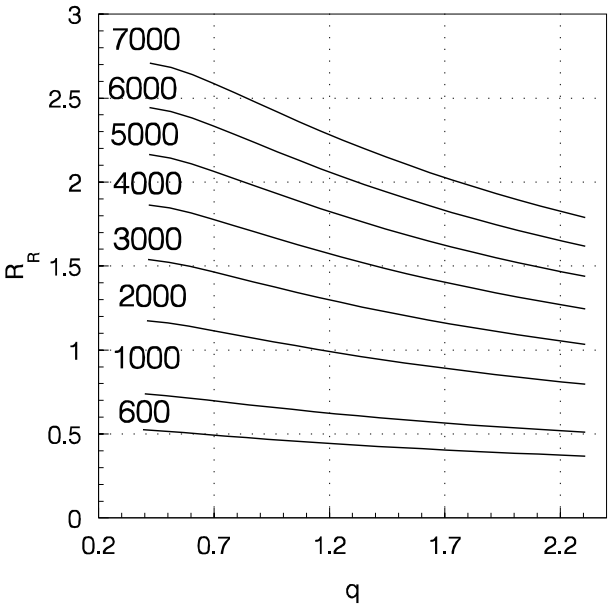

Fig. 4. Evolution of the Roche lobe radius R_R in AU (solid lines) for the different final orbital periods during the process of mass loss by wind as a function of the mass ratio q. The final values of orbital periods (in days) are indicated.

is more difficult to occur the Roche lobe overflow scenario, so that the circular orbit forms with more difficulties.

5. Conclusions and discussion

Taking the conservation of angular momentum in place of the conservation of tangential momentum for wind accretion scenario, and considering the square and higher power terms of orbital eccentricity, the change equations of orbital elements have been recalculated. These equations have been applied to quantitatively calculate the orbital elements of barium stars and to discuss the stellar wind accretion scenario.

Our results show that during the wind accretion process, the system widens as it loses mass, the orbital semi-major axis A will increase, resulting in an increase in the orbital period, which is similar to the result of Boffin & Jorissen (1988), but the eccentricity is very nearly constant. In general, barium stars evolved from normal G, K giants, namely, barium stars formed by accreting the ejecta of the G, K giant companions of binary systems. If the accretion is through stellar wind, the orbital period will increase and eccentricity remains nearly constant. Thus, for the same eccentricity, the orbital periods of barium stars are longer than those of normal G, K giants; while for the same orbital period, the maximum and average eccentricity of barium stars are lower than the corresponding values of the normal G, K giants. Our results can explain quantitatively these relations. Namely, we can explain the properties of (e,log$P$) diagrams of normal cluster giants and barium stars shown in Sect. 2.

(1) Eq. (2) represents the change of orbital semi-major axis A, which shows that A will increase during the wind accretion process, resulting the increase of orbital periods. But the orbital eccentricity will be very nearly constant with the wind accretion

(see Eq. (3) and Table 1). These results quantitatively explain the observational fact that the maximum eccentricities of barium stars is lower than the corresponding maximum eccentricities of normal giants at any given orbital periods.

(2) Regarding the maximum eccentricity line of normal G, K giants as the initial condition of a binary system, the maximum eccentricity line of barium stars can be obtained through the wind accretion calculation, which can fit the observations. Moreover, the two maximum eccentricity lines are near parallel (see Fig. 1 and Fig. 2).

(3) The average orbital eccentricity line of barium stars can be obtained through the wind accretion calculation, and can fit the observations. Namely, adopting η=0.685 for Eq. (11) of Boffin et al. (1993) to obtain the average eccentricities of barium stars, the initial eccentricities of binary systems can be obtained using our wind accretion model, which nearly overlap the observed average values of normal G, K giants given by Boffin et al. (1993) (see Fig. 3).

(4) For the low eccentricity systems, the observed maximum orbital period of circular orbits is $\sim$350 days for the cluster giants. Our result shows that this upper bound will lead to the corresponding maximum circular orbital period near 2000 days for barium stars using the wind accretion model, which can fit the observations. The threshold periods of CH and S stars are very similar to that of barium stars.

(5) Taking the highest orbital eccentricity 0.9 of normal G, K giants as the initial condition, we can calculate a large eccentricity, up to 0.9, for barium stars. The reason may be that the orbital period increases, but the eccentricity is nearly constant during the wind accretion process, so that the long orbital period and high eccentricity barium systems are formed. Our results can quantitatively explain the observed large eccentricity, 0.9, of some barium systems.

These fits between our results and the corresponding observations show that barium systems evolved from the normal G, K giants, and the distribution of orbital eccentricity with orbital period of barium stars can reflect the final orbital properties of binary systems through wind accretion for the binaries with longer period (P>1600 d).

Moreover, this period value can be understood roughly by the results shown in Fig. 4. Fig. 4 shows the evolution of Roche radius as a function of mass ratio q=M_1/M_2. The wind accretion scenario needs a larger Roche radius than the stellar radii of the previous primary stars of the binary systems, AGB stars. If we also consider the radii of AGB stars: a typical AGB star with log$T_{\rm eff}$=3.5 and $M_{\rm bol}$=$-$5 has a radius of 280$R_\odot$ (Jorissen & Boffin 1992), the comparison between the evolution of the radii of the AGB stars and the evolution of the Roche radii will show that the Roche radii are larger than the corresponding stellar radii for the binary systems with longer final orbital period (P>1600 d) during the binary evolutions. This result reflect that the barium stars with longer orbital period (P>1600 d) form through the wind accretion scenario.

In addition, Liang et al. (2000) confirmed this orbital period value taking advantage of the observational heavy element abundances of barium stars.

For the barium systems with shorter orbital periods, our wind accretion model is not sufficient to explain the observed properties. They may be formed through dynamical stability case C Roche lobe overflow, or common envelope ejection, or some other scenarios (Jorissen et al. 1995; Jorissen et al. 1998; Han et al. 1995 and references therein). Among the binary systems with shorter periods, the primary star may fill the Roche radius when it evolve to AGB phase, thus the mass-transfer process occur, but the previously strong wind mass loss has made the mass of primary star become very small so that mass ratio q (=M_1/M_2) is lower than a threshold value $q_{\rm crit}$ ($\sim$0.65, Pastetter & Ritter 1989), which causes the dynamically stable RLOF. While if the mass ratio q is greater than the $q_{\rm crit}$ when the primary AGB star fills its Roche lobe, the Roche lobe overflow will be dynamically unstable, leading to the formation of common envelope. Friction between the stars and the common envelope causes contraction of the binary orbit and release of energy. Most of the energy is used in the ejection of the common envelope. The binary after the ejection of common envelope comprises a white dwarf and a barium star with accreted neutron capture process elements$-$rich material. For such a binary, the orbital period and eccentricity are lower. The barium star HD 77247 ($P = 80.53$ d, $e = 0.09$) can be explained by the common envelope scenario.

Acknowledgements. We thank the anonymous referee for very useful suggestions on the original manuscript. We thank Dr. Alain Jorissen for fruitful discussion and warm-hearted help. Thank Dr. John Lattanzio for sending important material to us. This research work is supported by the National Natural Science Foundation of China under grant No. 19973002.

Appendix: derivation of Eq. (2) and Eq. (3)

For the binary system, the two components (an intrinsic AGB star with mass M_1, the present white dwarf star, and a main sequence star with mass M_2, the present barium star) rotating around the mass core C, so the total angular momentum is conservative in the mass core reference frame. If the mass exchange between the two components is wind accretion, the total angular momentum conservation is shown by:

$$\Delta(\mu r^2\dot{\theta}) = \omega r_1^2(\Delta M_1 + \Delta M_2) + r_2 v(\Delta M_1 + \Delta M_2), \quad \text{(A.1)}$$

where μ is reduced mass, and r is the distance from M_2 to M_1. r_1 and r_2 are the distances from M_1, M_2 to the mass core C respectively. ω (=$2\pi/P$) is angular velocity, where P=$2\pi A^2(1-e^2)^{\frac{1}{2}}/h$ is the orbital period (Huang 1956). v is an additional effective velocity defined through the angular momentum variation in the direction of orbital motion of component 2. The first term on the right side of the equal-sign is the angular momentum lost by the escaping material and the second term is the additional angular momentum lost by the escaping material.

For the binary system, according to Huang (1956), the changes of orbital elements, the orbital semi-major axis A and eccentricity e, are

$$\frac{\Delta A}{A} = \frac{\Delta(M_1+M_2)}{M_1+M_2} - \frac{\Delta E}{E}, \tag{A.2}$$

$$\frac{e\Delta e}{1-e^2} = \frac{\Delta(M_1+M_2)}{M_1+M_2} - \frac{1}{2}\frac{\Delta E}{E} - \frac{\Delta h}{h}, \tag{A.3}$$

where

$$\begin{aligned}\frac{\Delta E}{E} &= \frac{\Delta T}{E} + \frac{\Delta\Omega}{E} \\ &= \frac{r\dot\theta}{E}\Delta(r\dot\theta) + \left[\frac{\Delta(M_1+M_2)}{M_1+M_2}\frac{2A}{r} - \frac{2A\Delta r}{r^2}\right]. \end{aligned}\tag{A.4}$$

According to the angular momentum conservation model, the $\Delta(r\dot\theta)$ term can be obtained from the following equation:

$$\begin{aligned}&\frac{M_1M_2}{M_1+M_2}r\Delta(r\dot\theta) \\ &= \Delta\left(\frac{M_1M_2}{M_1+M_2}r\, r\dot\theta\right) - \Delta\left(\frac{M_1M_2}{M_1+M_2}r\right)\, r\dot\theta \\ &= \Delta(\mu r^2\dot\theta) - \Delta\left(\frac{M_1M_2}{M_1+M_2}r\right)\, r\dot\theta \\ &= \omega r_1^2(\Delta M_1+\Delta M_2) + r_2 v(\Delta M_1+\Delta M_2) \\ &\quad - \Delta\left(\frac{M_1M_2}{M_1+M_2}r\right)\, r\dot\theta, \end{aligned}\tag{A.5}$$

thus

$$\begin{aligned}\Delta(r\dot\theta) &= -r\dot\theta\left[\frac{\Delta M_1}{M_1}+\frac{\Delta M_2}{M_2}-\frac{\Delta(M_1+M_2)}{M_1+M_2}\right] - r\dot\theta\frac{\Delta r}{r} \\ &\quad + \frac{\Delta(M_1+M_2)}{M_2}v + \frac{rG^{\frac{1}{2}}M_2\Delta(M_1+M_2)}{M_1(M_1+M_2)^{\frac{1}{2}}A^{\frac{3}{2}}}, \end{aligned}\tag{A.6}$$

then, we can obtain

$$\begin{aligned}\frac{r\dot\theta\Delta(r\dot\theta)}{E} &= -\frac{(r\dot\theta)^2}{E}\left[\frac{\Delta M_1}{M_1}+\frac{\Delta M_2}{M_2}-\frac{\Delta(M_1+M_2)}{M_1+M_2}\right] \\ &\quad - \frac{r\dot\theta^2}{E}\Delta r + \frac{r\dot\theta}{E}\frac{\Delta(M_1+M_2)}{M_2}v \\ &\quad + \frac{r^2\dot\theta}{E}\frac{G^{\frac{1}{2}}M_2\Delta(M_1+M_2)}{M_1(M_1+M_2)^{\frac{1}{2}}A^{\frac{3}{2}}} \\ &= 2(1-e^2)^{\frac{1}{2}}\left[\frac{\Delta M_1}{M_1}+\frac{\Delta M_2}{M_2}-\frac{\Delta(M_1+M_2)}{M_2}\frac{v}{v_{\rm orb}}\right] \\ &\quad - 2(1-e^2)^{\frac{1}{2}}\frac{M_2\Delta(M_1+M_2)}{M_1(M_1+M_2)} \\ &\quad - 2(1-e^2)^{\frac{1}{2}}\frac{\Delta(M_1+M_2)}{M_1+M_2} + \frac{h\dot\theta\Delta r}{Er} \\ &= 2(1-e^2)^{\frac{1}{2}}\left[\frac{\Delta M_1}{M_1}+\frac{\Delta M_2}{M_2}-\frac{\Delta(M_1+M_2)}{M_2}\frac{v}{v_{\rm orb}}\right] \\ &\quad - 2(1-e^2)^{\frac{1}{2}}\frac{M_2\Delta(M_1+M_2)}{M_1(M_1+M_2)} \\ &\quad - 2(1-e^2)^{\frac{1}{2}}\frac{\Delta(M_1+M_2)}{M_1+M_2} + \frac{2\Delta r}{A(1-e^2)^{\frac{1}{2}}}. \end{aligned}\tag{A.7}$$

Thus

$$\begin{aligned}\frac{\Delta E}{E} &= 2(1-e^2)^{\frac{1}{2}}\left[\frac{\Delta M_1}{M_1}+\frac{\Delta M_2}{M_2}-\frac{\Delta(M_1+M_2)}{M_2}\frac{v}{v_{\rm orb}}\right] \\ &\quad - 2(1-e^2)^{\frac{1}{2}}\frac{M_2\Delta(M_1+M_2)}{M_1(M_1+M_2)} \\ &\quad + (2-2(1-e^2)^{\frac{1}{2}})\frac{\Delta(M_1+M_2)}{M_1+M_2}. \end{aligned}\tag{A.8}$$

The $\Delta h/h$ term can be obtained from:

$$\begin{aligned}\Delta(\mu r^2\dot\theta) &= \Delta(\mu h) \\ &= \Delta(\frac{M_1M_2}{M_1+M_2}h) \\ &= \Delta(\frac{M_1M_2}{M_1+M_2})h + \frac{M_1M_2}{M_1+M_2}\Delta h \\ &= \omega r_1^2\Delta(M_1+M_2) + r_2 v\Delta(M_1+M_2), \end{aligned}\tag{A.9}$$

and

$$\begin{aligned}\frac{\Delta h}{h} &= -\frac{\Delta M_1}{M_1} - \frac{\Delta M_2}{M_2} + \frac{2+e^2}{2(1-e^2)^{\frac{1}{2}}}\frac{\Delta(M_1+M_2)}{M_2}\frac{v}{v_{\rm orb}} \\ &\quad + \frac{M_2\Delta(M_1+M_2)}{M_1(M_1+M_2)} + \frac{\Delta(M_1+M_2)}{M_1+M_2}. \end{aligned}\tag{A.10}$$

Combining Eqs. (A.2), (A.3), (A.8) and (A.10), we can obtain the changes of orbital semi-major axis A and eccentricity e:

$$\begin{aligned}\frac{\Delta A}{A} &= -2(1-e^2)^{\frac{1}{2}}\left[\frac{\Delta M_1}{M_1}+\frac{\Delta M_2}{M_2}-\frac{\Delta M_1+\Delta M_2}{M_2}\frac{v}{v_{\rm orb}}\right] \\ &\quad + 2(1-e^2)^{\frac{1}{2}}\frac{M_2(\Delta M_1+\Delta M_2)}{M_1(M_1+M_2)} \\ &\quad + [2(1-e^2)^{\frac{1}{2}}-1]\frac{\Delta M_1+\Delta M_2}{M_1+M_2}, \end{aligned}\tag{A.11}$$

$$\begin{aligned}\frac{e\Delta e}{1-e^2} &= [1-(1-e^2)^{\frac{1}{2}}]\left[\frac{\Delta M_1}{M_1}+\frac{\Delta M_2}{M_2}-\frac{\Delta M_1+\Delta M_2}{M_1+M_2}\right] \\ &\quad - [1-(1-e^2)^{\frac{1}{2}}]\frac{M_2(\Delta M_1+\Delta M_2)}{M_1(M_1+M_2)} \\ &\quad - \frac{3e^2}{2(1-e^2)^{\frac{1}{2}}}\frac{\Delta M_1+\Delta M_2}{M_2}\frac{v}{v_{\rm orb}}. \end{aligned}\tag{A.12}$$

For obtaining the above equations, averaging over the orbital period then amounts to using the following mean values:

$$\left\langle\frac{\dot\theta}{r}\right\rangle = \frac{2\pi}{PA(1-e^2)}$$

$$\langle r\rangle = A(1+\frac{1}{2}e^2)$$

$$\left\langle r\dot\theta\right\rangle = \frac{2\pi A(1-e^2)^{\frac{1}{2}}}{P}$$

$$\left\langle\dot\theta\right\rangle = \frac{2\pi}{P}$$

$$\left\langle (r\dot{\theta})^2 \right\rangle = (\frac{2\pi A}{P})^2 (1-e^2)^{\frac{1}{2}}$$

$$\left\langle \frac{1}{r} \right\rangle = \frac{1}{A}$$

$$\left\langle \frac{1}{r^2} \right\rangle = \frac{1}{A^2(1-e^2)^{\frac{1}{2}}}$$

References

Boffin H.M.J., Cerf N., Paulus G., 1993, A&A 271, 125
Boffin H.M.J., Jorissen A., 1988, A&A 205, 155
Boffin H.M.J., Začs L., 1994, A&A 291, 811
Böhm-Vitense E., Carpenter K. Robinson R., Ake T., Brown J., 2000 ApJ 633, 969
Chang Rui-xiang, Zhang Bo, Peng Qiu-he, 1997, Chin. Astron. Astrophys. 21, 453
Han Z., Eggleton P.P., Podsiadlowski P., Tout C.A., 1995, MNRAS 277, 1443
Huang S.S., 1956, AJ 61, 49
Iben I. Jr., Tutukov A.V., 1985, ApJS 58, 661
Jorissen A., 1999, In: Le Bertre T., Lébre A., Waelkens C. (eds.) Asymptotic Giant Branch Stars. IAU Symp. 191, ASP, p. 437
Jorissen A., Boffin H.M.J., 1992, In: Duquennoy A., Mayor M. (eds.) Binaries as Tracers of Stellar Formation. Cambridge University Press, Cambridge, p. 110
Jorissen A., Hennen O., Mayor M., Bruch A., Sterken Ch., 1995, A&A 301, 707
Jorissen A., Mayor M., 1992, A&A 260, 115
Jorissen A., Van Eck S., 2000, In: Wing R.F. (ed.) The Carbon Star Phenomenon. IAU Symp. 177, ASP, San Francisco, astro-ph/9708052
Jorissen A., Van Eck S., Mayor M., Udry S., 1998, A&A 332, 877
Karakas A.I., Tout C.A., Lattanzio J.C., 2000 MNRAS 316, 689
Liang Y.C., Zhao G., Zhang B., 2000, A&A (in press)
Mermilliod J.-C., 1996, In: Milone G., Mermilliod J.-C. (eds.) The Origins, Evolution, and Destinies of BinaryStars in Clusters. ASP Conf. Ser., p. 95
McClure R.D., Fletcher J.M., Nemec J.M., 1980, ApJ 238, L35
Paczynski B., 1976, In: Eggleton P.P., Mitton S., Whelan J. (eds.) IAU Symp. 73, Structure and Evolution of Close Binary Systems. Reidel, Dordrecht, p. 75
Pastetter L., Ritter H., 1989, A&A 214, 186
Theuns T., Boffin H.M.J., Jorissen A., 1996 MNRAS 280, 1264
Začs L., 1994, A&A 283, 937
Zhang Bo, Chang Rui-xiang, Peng Qiu-he, 1998, Chin. Astron. Astrophys. 22, 49
Zhang Bo, Liu Jun-hong, Liang Yan-chun, Peng Qiu-he, 1999, Chin. Astron. Astrophys. 23, 189